Published in final edited form as:
Hepatology. 2010 September ; 52(3): 945–953. doi:10.1002/hep.23748.

Epithelial-to-Mesenchymal Transition of Murine Liver Tumor Cells Promotes Invasion

Wei Ding[1], **Hanning You**[1], **Hien Dang**[1], **Francis LeBlanc**[1], **Vivian Galicia**[2], **Shelly C. Lu**[3], **Bangyan Stiles**[2], and **C. Bart Rountree**[1]

[1]Department of Pediatrics and Pharmacology, The Pennsylvania State University College of Medicine, Hershey, PA

[2]Department of Pharmacology and Pharmaceutical Sciences, University of Southern California, Los Angeles, CA

[3]Division of Gastroenterology and Liver Diseases, USC Research Center for Liver Disease, The Southern California Research Center for ALPD and Cirrhosis, Keck School of Medicine, University of Southern California, Los Angeles, CA

Abstract

Epithelial-to-mesenchymal transition (EMT) is predicted to play a critical role in metastatic disease in hepatocellular carcinoma. In this study, we used a novel murine model of EMT to elucidate a mechanism of tumor progression and metastasis. A total of 2×10^6 liver cells isolated from *Pten*$^{loxp/loxp}$/*Alb-Cre*$^{+}$ mice, expanded from a single CD133^{+}CD45^{-} cell clone, passage 0 (P0), were sequentially transplanted to obtain two passages of tumor cells, P1 and P2. Cells were analyzed for gene expression using microarray and real-time polymerase chain reaction. Functional analysis included cell proliferation, migration, and invasion in vitro and orthotopic tumor metastasis assays in vivo. Although P0, P1, and P2 each formed tumors consistent with mixed liver epithelium, within the P2 cells, two distinct cell types were clearly visible: cells with epithelial morphology similar to P0 cells and cells with fibroblastoid morphology. These P2 mesenchymal cells demonstrated increased locomotion on wound healing; increased cell invasion on Matrigel basement membrane; increased EMT-associated gene expression of *Snail1, Zeb1, and Zeb2*; and down-regulated *E-cadherin*. P2 mesenchymal cells demonstrated significantly faster tumor growth in vivo compared with P2 epithelial counterparts, with invasion of intestine, pancreas, spleen, and lymph nodes. Furthermore, P2 mesenchymal cells secreted high levels of hepatocyte growth factor (HGF), which we propose acts in a paracrine fashion to drive epithelial cells to undergo EMT. In addition, a second murine liver cancer stem cell line with methionine adenosyltransferase 1a deficiency acquired EMT after sequential transplantations, indicating that EMT was not restricted to Pten-deleted tumors.

Conclusion—EMT is associated with a high rate of liver tumor proliferation, invasion, and metastasis in vivo, which is driven by HGF secreted from mesenchymal tumor cells in a feed-forward mechanism.

Address reprint requests to: C. Bart Rountree, M.D., Department of Pediatrics and Pharmacology, The Pennsylvania State University College of Medicine, 500 University Drive, H085, Hershey, PA 17033. crountree@hmc.psu.edu; fax: 717-531-0653.

Microarray data are available at www.ncbi.nlm.nih.gov/geo/Accession Number GSE18255.

Potential conflict of interest: Nothing to report.

Additional Supporting Information may be found in the online version of this article.

Hepatocellular carcinoma (HCC) represents the third leading cause of cancer-related mortality worldwide.[1,2] Despite many scientific advances, the prognosis for many HCC patients remains poor due to intrahepatic and extrahepatic metastasis and postsurgical recurrence.3 The pathogenesis of HCC progression and metastasis is not well defined, further contributing to the lack of effective therapeutics for advanced HCC.4

Growing evidence indicates that the epithelial-to-mesenchymal transition (EMT) of epithelial cancers correlates with aggressive tumors in HCC patients. EMT represents a change from stationary, polarized epithelial cells organized in stratum to single fibroblastoid cells capable of locomotion.[4] EMT was originally described during embryonic development[4,5] and is hypothesized to play a role in metastatic cancers.[4,6] For example, up-regulation of *Twist*, a transcription factor that drives EMT, correlates with HCC cell invasion and metastasis.[7–9] In addition, hepatitis C virus core protein is able to shift the transforming growth factor-β (TGF-β) response from tumor suppression to EMT, a potential contribution to metastasis in HCC.[10]

EMT is characterized by decreased cell adhesion, which is accompanied by the down-regulation of E-cadherin, an epithelial adhesion protein.[6,11] EMT is regulated by several transcription factors, including Snail, Slug, Zeb1, Zeb2, Twist1/2, and E12/E47, each of which bind the *E-cadherin* promoter and repress transcription.[6,11,12] A variety of signaling pathways are involved in the initiation and maintenance of EMT, including TGF-β and hepatocyte growth factor (HGF).[6,12] However, the mechanism underlying the acquisition of EMT and the role of EMT in the promotion of HCC metastasis remains poorly understood. In the present study, we explored EMT as a mechanism for tumor progression of cancer stem cell (CSC)-derived tumors. We used liver CSCs that were isolated from two liver disease models, one of which lacked the tumor suppressor phosphatase and tensin homolog deleted on chromosome 10 (Pten).[13,14] Loss or reduction of Pten has been strongly correlated with aggressive forms of liver cancer.15

In the present study, we established an EMT model of liver cancer generated from sequentially transplanted cells expanded from a single $CD133^+$ CSC clone and determined the contribution of two distinct cell types—epithelial and mesenchymal tumor cells—to liver cancer growth and metastasis. In addition, our results indicate that dysregulation of the HGF signaling pathway may play a role in the promotion of metastatic disease.

Materials and Methods

Cell Culture

Pten$^{-/-}$ cells and methionine adenosyltransferase 1a–deficient (*MAT1a*$^{-/-}$) cells expanded from single $CD133^+$ cells and isolated from sequentially transplanted tumors were cultured in Dulbecco's modified Eagle's medium (DMEM)/F12 at 1:1 medium (Mediatech, Manassas, VA) with 10% fetal bovine serum as described.[13,14]

Nude Mice

Mice were fed ad libitum (Harlan Teklad irradiated mouse diet 7912, Madison, WI) and housed in a temperature-controlled animal facility with a 12-hour light/dark cycle. All procedures were in compliance with our institution's guidelines for the use of laboratory animals and approved by the Institutional Animal Care and Use Committee.

Genotyping

Genomic DNA was isolated using Wizard SV Genomic DNA purification system (Promega, Madison, WI). Genotyping was performed as described using the primers listed in Supporting Information Fig. 1.[16]

Real-Time Polymerase Chain Reaction

Real-time polymerase chain reaction (PCR) experiments were conducted as described.[13] The housekeeping gene *GAPDH* was used for ΔΔCt calculations (see Supporting Information Methods for details).

Cell Proliferation Assays

Cell proliferation was analyzed using the XTT [2,3-bis(2-methoxy-4-nitro-5-sulfophenyl)-2H-tetrazolium-5-carboxanilide] kit from Trevigen (Gaithersburg, MD) according to the manufacturer's protocol. A total of 5×10^3 cells/well were plated in 96-well plates. Cells were treated in serum-free medium for 1 hour and incubated with HGF for an additional 24 hours.

Western Blot Analysis

Protein from cell lysates was harvested and processed as described13,[17] (see Supporting Information Methods for details).

Cell Migration Assay

The capability of tumor cell migration was assessed using a wound-healing assay. Confluent cell monolayers were manually wounded by scraping the cells with a 1,000 μL pipette tip. The cell culture medium was replaced and migration was assessed at 18 hours.

Basement Membrane Invasion Assay

Cell invasion was assessed using 6-well Transwell permeable inserts with 8-μm pores (Corning, Corning, NY).[18] In brief, 1×10^5 cells were cultured in a serum-free DMEM/F12 on an insert coated with Matrigel (BD, Franklin Lakes, NJ). Below the insert, the chamber of 6-well plates contained DMEM/F12 supplemented with 10% fetal bovine serum. Cells were incubated in a cell culture incubator for 48 hours. After fixation and staining, the number of cells that invaded across the membranes was counted.

HGF Enzyme-Linked Immunosorbent Assay

A total of 5×10^6 cells were cultured in 4 ml of serum-free DMEM/F12 in 100-mm culture dishes for 48 hours and conditioned medium was collected. The HGF concentration was measured using a rat/mouse HGF enzyme-linked immunosorbent assay kit purchased from B-Bridge International (Mountain View, CA) per the manufacturer's protocol.

Microarray Analysis

Using the *Pten*$^{-/-}$ model, P0, P1, P2, P2E (P2 epithelial subfraction), and P2M (P2 mesenchymal subfraction) messenger RNA were analyzed using an Illumina (San Diego, CA) mouse gene chip according to the manufacturer's protocol and as described.[13,19] Housekeeping genes were used as standards to generate expression levels, and data analysis was conducted using 1.4-fold or greater change in expression with $P < 0.05$ as significant. The full complement of the expression data is available at http://www.ncbi.nlm.nih.gov/geo (accession number GSE18255).

Luciferase Retrovirus Cell Infection

See Supporting Information Methods.

Tumorigenicity Assay

Cells were counted with trypan blue exclusion[13] and were resuspended in phosphate-buffered saline (PBS) for transplantation at a concentration of 2×10^6 live cells/200 μL (1:1 Matrigel/Dulbecco's PBS). Six-week-old female nude mice (The Jackson Laboratory, Bar Harbor, ME) were used for all tumor assays. Nude mice were subcutaneously inoculated.[13] Tumor dimensions were measured with calipers.

Orthotopic Transplantation

Nude mice were anesthetized with 100 mg/kg of ketamine and 10 mg/kg of xylazine, and the liver was exposed through a surgical incision. A total of 3×10^5 cells in 30 μL Dulbecco's PBS were orthotopically inoculated. To avoid tumor cell leakage, pressure was applied to the injection site for 2 minutes.

Bioluminescent Image Collection

Nude mice were anesthetized at defined times after cell transplantation, and 150 mg/kg of luciferin was injected intraperitoneally. Ten minutes after luciferin injection, bioluminescence images were collected using a Xenogen IVIS 50 system according to the manufacturer's instructions.

Statistical Analyses

For nonmicroarray analysis, a paired two-tailed Student *t* test was used when comparing two groups. One-way analysis of variance was applied when comparing multiple groups. $P < 0.05$ was considered statistically significant.

Results

Cells Expanded from CD133$^+$ Liver CSCs Acquire EMT

In our previous studies, we reported that CD133$^+$ liver stem cells isolated from *Pten*$^{loxp/loxp}$/*Alb-Cre*$^+$ mice represent liver CSCs.[13] These CSCs initiate HCC-like and cholangiocarcinoma-like tumors in vivo. In order to further define the role of liver CSCs in HCC progression, we performed sequential transplantation (Fig. 1). A total of 2×10^6 cells (in vivo passage 0), expanded from CD133$^+$ CSCs, were subcutaneously transplanted into immune-deficient mice. We define passage to mean transplantation; thus passage 0 (P0) cells, isolated from the original *Pten*$^{-/-}$ mice, have not been transplanted. The tumors that resulted from P0 transplantations were dissected for re-expansion in vitro as P1 cells (the first round of transplantation). A second-round subcutaneous transplantation using P1 cells resulted in tumors that yielded P2 cells. Within P2 cells, two distinct cell types were visible. One cell type had a cobblestone morphology characteristic of liver epithelial cells. A second group demonstrated elongated spindle-like morphology. Because the P2 cells contained a mixture of epithelial and mesenchymal cells, clones of these two cell populations were subisolated using two rounds of sequential trypsinization and expanded as P2E (epithelial) and P2M (mesenchymal) cells (Fig. 1).

To confirm that the mesenchymal cells were not a result of contamination from the host fibroblast cells, we performed genotyping and western blot assays. As shown in Supporting Information Fig. 2A, all P0, P1, P2, P2E, and P2M cells demonstrated a 300-bp PCR fragment with a deletion of *Pten* exon 5. The 500-bp fragment representing wild-type *Pten* was detectable in host mice. Western blot analysis demonstrated that PTEN protein was

detectable in wild-type control cells, but not in P0, P1, P2, P2E, and P2M cells. Each of the *Pten*$^{-/-}$ cells demonstrated constitutive phosphorylation of Akt (Supporting Information Fig. 2B). In addition, we isolated mesenchymal tumor cells using laser capture microdissection from P2 tumors to confirm a *Pten*$^{-/-}$ genotype (Supporting Information Fig. 3). These results confirmed that the mesenchymal tumor cells were derived from the original *Pten*$^{-/-}$ model.

In order to confirm that P2M cells possess a mesenchymal phenotype, we analyzed the gene expression profiles of P2E and P2M cells. As shown in Fig. 2A, numerous epithelial cell–related genes, including *E-cadherin* (*Cdh1*), *Claudin3* (*Cldn3*), and *keratins* (*Krt8, Krt14, Krt18*, and *Krt19*), were significantly down-regulated, whereas several mesenchymal cell markers (such as *Mmp2/3, Snail1, Zeb1*, and *Zeb2*) were significantly up-regulated in P2M cells compared with P2E cells. We validated microarray results using real-time PCR for *E-cadherin, Snail1, Zeb1*, and *Zeb2* expression, as shown in Fig. 2B.

To further confirm that E-cadherin was down-regulated in P2M cells, we performed immunofluorescent staining. As shown in Fig. 3A, P2E cells demonstrated abundant expression of E-cadherin in a cell surface pattern. In contrast, P2M cells demonstrated lower levels of E-cadherin staining. Immunohistochemical staining of mixed morphology P2 tumors demonstrated that E-cadherin was absent in the mesenchymal areas of the tumor (Fig. 3B).

To verify our findings, we repeated the original transplantation of P1 cells 10 additional times. We found that all tumors (100%) demonstrated mixed epithelial and mesenchymal cells as shown by both hematoxylin-eosin staining and cell morphology (Supporting Information Fig. 4A,B). We tested multiple sections of each tumor, and all sections tested demonstrated *Pten*$^{-/-}$ status (Supporting Information Fig. 4C). It should be noted that mesenchymal cells were generated after in vivo transplantation and not during in vitro culture. P0, P1, and P2E cells maintained epithelial morphology in vitro after 20 passages.

HGF Secreted by Mesenchymal Cells Induces EMT

In our gene expression profile, we discovered significant changes in several genes in P2M cells, including *HGF*. In this analysis, *HGF* was increased 2.4-fold in P2M cells compared with P2E (GEO accession #GSE18255). The HGF signaling pathway has been shown to play an important role in the induction of EMT in several cell types,[20] and overexpression of HGF/c-Met signals is highly correlated with recurrence and poor survival in patients with HCC.21 High *HGF* expression in P2M cells was confirmed with *HGF*-specific reverse-transcription PCR (Fig. 4A, Supporting Information Fig. 5A). To determine whether HGF was secreted by mesenchymal cells, we measured HGF protein concentration in serum-free conditioned medium (CM). As shown in Fig. 4B, CM collected from P2M cells contained a high concentration of HGF (1 ng/mL) compared with P0, P1, and P2E cells. We reported previously that P0 cells have high *c-Met* expression,[13] and we have confirmed expression of *c-Met* in P0, P1, P2, P2E, and P2M cells (data not shown).

Because many reports indicate that HGF induces EMT, we proposed a positive feed-forward loop between epithelial cells and the mesenchymal cells. In our proposed model, HGF secreted by mesenchymal cells acts in a feed-forward manner on epithelial cells to promote cell proliferation and EMT. To test this hypothesis, we treated P2E cells with recombinant HGF. In this system, HGF stimulation promoted epithelial cell proliferation (Supporting Information Fig. 5B). In addition, HGF stimulation results in a morphological change from epithelial cells to fibroblastoid cells (Fig. 4C). HGF-induced EMT was confirmed with a significant down-regulation of *E-cadherin* and up-regulation of *Zeb1* and *Zeb2* (Fig. 4D, Supporting Information Fig. 5C).

In addition to testing recombinant HGF, we examined the effect of CM collected from P2M cells. As with HGF, P2M CM promoted P2E cell proliferation (Supporting Information Fig. 5D). Moreover, P2M CM was able to promote P2E cells to undergo EMT, as measured by morphological change, up-regulation of *Zeb1* and *Zeb2*, and down-regulation of *E-cadherin* (Fig. 4E,F).

Acquisition of EMT Promotes Tumor Growth In Vivo

To further understand whether acquisition of EMT is able to promote tumor growth in vivo, we performed a subcutaneous tumor growth assay using nude mice. As shown in Fig. 5A, P2 and P2M cells generated tumors significantly larger than those of P0, P1, and P2E cells. Histological examination demonstrated that P1 and P2E cells generated uniform hepatoma-like tumors, whereas P2M cells formed fibroblastoma-like tumors, and tumors generated by P2 cells demonstrated both epithelial and mesenchymal cell morphologies (Fig. 5B). Staining tumors demonstrated that the epithelial components contained hepatocyte-like and cholangiocyte-like features (Supporting Information Figs. 6 and 7).

Mesenchymal Cells Demonstrate Migration and Invasion In Vitro

To determine whether mesenchymal cells are more invasive in vitro compared with epithelial cells, we used migration and invasion assays. Compared with epithelial P0, P1, and P2E cells, significantly more mesenchymal P2M cells migrated into the wound area (Fig. 6A). In addition, significantly more mesenchymal P2M cells invaded through Matrigel pores compared with epithelial P0, P1, and P2E cells (Fig. 6B).

Acquisition of EMT Promotes Metastasis In Vivo

To test whether cells with mesenchymal phenotype are able to invade tissue and metastasize in vivo, 3×10^5 of P0, P2E, and P2M cells with stable expression of luciferase were orthotopically transplanted into the livers of nude mice. As demonstrated in Fig. 7A, P0 and P2E tumor growth was restricted to the site of transplantation in the liver. P2M tumors formed large intrahepatic tumors and seeded tumors throughout the peritoneal cavity. In fact, the level of bioluminescence data collected between groups was large enough at 2 weeks that we were unable to perform comparative analysis (P2M tumors were saturated in the imaging system after 15 seconds, and the P0 and P2E tumors were detectable only after 20 seconds). In addition, P2M cells grossly invaded multiple abdominal organs, including the pancreas and intestine, as well as the spleen and lymph nodes. Histological examination demonstrated numerous intrahepatic metastatic lesions, tumor invasion of pancreatic tissue and colonic tissue, metastatic lesions within the spleen and lymph nodes, and tumor invasion of abdominal wall muscle (Fig. 7B–G). These findings support the hypothesis that tumor cells that acquire EMT are important for invasion and metastasis.

A Second Model of EMT with Wild-Type Pten

In order to examine whether EMT can be induced in tumor cells with the wild-type *Pten* gene, we repeated sequential transplantations using *MAT1a*$^{-/-}$ murine liver cancer stem cells.[13,14] After two sequential transplantations, all *MAT1a*$^{-/-}$ P2 tumors (n = 9) demonstrated epithelial and mesenchymal cells on histological analysis of tumor tissue and morphological analysis of cells in vitro (Supporting Information Fig. 8A,B). To confirm that mesenchymal cells were derived from the original P0 *MAT1a*$^{-/-}$ cells, we performed genotyping analysis. As shown in Supporting Information Fig. 8C, the neomycin resistance gene was amplified in *MAT1a*$^{-/-}$ tumor cells along with the wild-type *Pten* gene, and the *MAT1a* gene was lacking in all *MAT1a*$^{-/-}$ cells. Within *MAT1a*$^{-/-}$ P2 tumors with mesenchymal cells, *E-cadherin* was significantly down-regulated and *N-cadherin* was significantly up-regulated. Using this model, we confirmed lower levels of E-cadherin

protein expression and increased *HGF* gene expression in *MAT1a*$^{-/-}$ P2 cells (Supporting Information Fig. 8E,F). Interestingly, there was no difference in the expression levels of *Snail*, *Zeb1*, or *Zeb2* between *MAT1a*$^{-/-}$ P0 and P2 cells (data not shown), indicating that EMT induction in *MAT1a*$^{-/-}$ cells may occur through a different mechanism than that in *Pten*$^{-/-}$ cells.

Discussion

In this study, we established a unique model of EMT through sequential transplantation using liver cells that were expanded from a *Pten*$^{-/-}$ CD133^{+} cells. For the first time, we report that EMT can be induced in an animal model without ectopic overexpression of EMT-related transcription factors (such as *Snail1* or *Twist1*) or exogenous treatment with EMT induction factors (such as HGF or TGF-β). We demonstrate that once tumor cells undergo EMT, they acquire the capability of migration and invasion both in vitro and in vivo. Our findings are consistent with recent HCC studies that demonstrate induction of EMT with loss of *E-cadherin* and subsequent metastasis with the up-regulation of *Snail* or *Twist*.[7,9,22–25]

Understanding the mechanism of EMT initiation will assist in the delineation of HCC tumor progression. In the present study, EMT did not occur in vitro, because we cultured *Pten*$^{-/-}$ and *MAT1a*$^{-/-}$ P0 and P1 epithelial cells more than 20 generations in vitro without any change in morphology or EMT-related gene expression. This finding indicates that the tumor microenvironment may play a critical role in the initiation of EMT. One potential process driving EMT is that stromal cells surrounding the tumor produce growth factors that can initiate EMT through intracellular signaling, such as the PI3 kinase and mitogen-activated protein kinase pathways.

In addition, based on recent reports, we propose that hypoxia may be a second factor in the initiation of EMT. Within human HCC cell lines, hypoxic conditions were able to induce EMT through up-regulation of phosphoinositide 3-kinase/Akt pathway activation.[26] Based on this report, unregulated phosphoinositide 3-kinase/Akt activity may be driving EMT within the *Pten*$^{-/-}$ model. Alternatively, up-regulation of the mitogen-activated protein kinase pathway may play an important role in the initiation of EMT in the *MAT1a*$^{-/-}$ cells. Our findings indicate that distinct intracellular mechanisms may be responsible for the induction of EMT within different HCC cells, which is supported by a recent review that proposes that numerous signaling pathways are independently involved in EMT.[12]

Our model is a novel one because after EMT, mesenchymal tumor cells secrete high levels of HGF that can then feed-forward tumor growth and continued EMT. The effect of HGF as a mitogen and migration inducer has been well documented.[27] In oval cells, HGF autocrine and paracrine stimulation has recently been demonstrated to be a mechanism of survival.[28] In terms of liver cancer patients, increased serum levels of HGF are associated with poor survival.[29] In addition, HGF stimulates the migration of HCC cells through the tyrosine phosphorylation of c-Met,[30] and autocrine and paracrine HGF stimulation play an important role in the development and metastatic potential of HCC.[31] Moreover, inhibition of the HGF/c-Met signal transduction system reduces HCC growth and metastasis.[31,32]

Some investigators have suggested that HGF is produced by the liver stellate or myofibroblast cells and not by HCC tumor cells.33–35 In the present study, HGF expression was restricted to mesenchymal tumor cells, indicating that tumor cells gained the function of HGF secretion after EMT. As depicted in Supporting Information Fig. 9, we propose that in the early stage of HCC, the tumor surrounding stellate and/or myofibroblast cells are the major cells responsible for the production of HGF or other molecules (TGF-β) that trigger

EMT, and once tumor cells acquired a mesenchymal phenotype, they produce more EMT-related growth factors such as HGF and further feed-forward epithelial cells to undergo EMT and promote HCC progression.

In the gene expression profiling data set of this study, we discovered a number of other growth factors, such as fibroblast growth factors (FGFs), were significantly up-regulated in mesenchymal cells compared with epithelial counterparts. Several FGF family members play a critical role in the induction and maintenance of EMT in several solid tumors.[36,37] In addition, serum basic FGF levels were highly correlated with tumor invasiveness and postresection recurrence of HCC,38 implying that more than one mitogenic pathway may be dysregulated after acquisition of EMT.

In conclusion, we have clearly demonstrated a model of liver cancer EMT, in which mesenchymal tumor cells secrete high levels of HGF resulting in rapid tumor growth and invasion in vivo.

Abbreviations

CM	conditioned medium
CSC	cancer stem cell
DMEM	Dulbecco's modified Eagle's medium
EMT	epithelial-to-mesenchymal transition
FGF	fibroblast growth factor
HCC	hepatocellular carcinoma
HGF	hepatocyte growth factor
MAT1a	methionine adenosyl transferase 1a
P	passage
PBS	phosphate-buffered saline
PCR	polymerase chain reaction
Pten	phosphatase and tensin homolog deleted on chromosome 10
TGF-β	transforming growth factor-β

Acknowledgments

We thank Drs. Robert Cooney and Mingjie Sun for technical assistance in transplantation models and acknowledge Drs. Kent Vrana and Willard Freeman of the Functional Genomics Core (The Pennsylvania State University College of Medicine). Important Functional Genomics Core Facility instrumentation purchases were made possible through Tobacco Settlement Funds and through a Penn State Cancer Institute contract with the Department of the Navy.

C. Bart Rountree was supported by National Institute of Diabetes and Digestive and Kidney Disorders (NIDDK) Grant K08DK80928; American Cancer Society Grant RSG-10-073-01-TBG; the Office for the Advancement of Telehealth, Health Resources and Services Administration, Department of Health and Human Services Grant D1BTH06321; the Children's Miracle Network; and a Penn State College of Medicine Barsumian Trust Award. Shelly Lu was supported by NIDDK Grant DK51719 and National Center for Complementary and Alternative Medicine Grant AT1576. Bangyan Stiles was supported by the NIDDK.

References

1. Parkin DM, Bray F, Ferlay J, Pisani P. Global cancer statistics, 2002. CA Cancer J Clin 2005;55:74–108. [PubMed: 15761078]
2. El-Serag HB, Marrero JA, Rudolph L, Reddy KR. Diagnosis and treatment of hepatocellular carcinoma. Gastroenterology 2008;134:1752–1763. [PubMed: 18471552]
3. Altekruse SF, McGlynn KA, Reichman ME. Hepatocellular carcinoma incidence, mortality, and survival trends in the United States from 1975 to 2005. J Clin Oncol 2009;27:1485–1491. [PubMed: 19224838]
4. Acloque H, Adams MS, Fishwick K, Bronner-Fraser M, Nieto MA. Epithelial-mesenchymal transitions: the importance of changing cell state in development and disease. J Clin Invest 2009;119:1438–1449. [PubMed: 19487820]
5. Nakaya Y, Sheng G. Epithelial to mesenchymal transition during gastrulation: an embryological view. Dev Growth Differ 2008;50:755–766. [PubMed: 19046163]
6. Kalluri R, Weinberg RA. The basics of epithelial-mesenchymal transition. J Clin Invest 2009;119:1420–1428. [PubMed: 19487818]
7. Matsuo N, Shiraha H, Fujikawa T, Takaoka N, Ueda N, Tanaka S, et al. Twist expression promotes migration and invasion in hepatocellular carcinoma. BMC Cancer 2009;9:240. [PubMed: 19615090]
8. Lee TK, Poon RT, Yuen AP, Ling MT, Kwok WK, Wang XH, et al. Twist overexpression correlates with hepatocellular carcinoma metastasis through induction of epithelial-mesenchymal transition. Clin Cancer Res 2006;12:5369–5376. [PubMed: 17000670]
9. Niu RF, Zhang L, Xi GM, Wei XY, Yang Y, Shi YR, et al. Up-regulation of Twist induces angiogenesis and correlates with metastasis in hepatocellular carcinoma. J Exp Clin Cancer Res 2007;26:385–394. [PubMed: 17987801]
10. Battaglia S, Benzoubir N, Nobilet S, Charneau P, Samuel D, Zignego AL, et al. Liver cancer-derived hepatitis C virus core proteins shift TGF-beta responses from tumor suppression to epithelial-mesenchymal transition. PLoS One 2009;4:e4355. [PubMed: 19190755]
11. Zeisberg M, Neilson EG. Biomarkers for epithelial-mesenchymal transitions. J Clin Invest 2009;119:1429–1437. [PubMed: 19487819]
12. Thiery JP, Acloque H, Huang RY, Nieto MA. Epithelial-mesenchymal transitions in development and disease. Cell 2009;139:871–890. [PubMed: 19945376]
13. Ding W, Mouzaki M, You H, Laird JC, Mato J, Lu SC, et al. CD133+ liver cancer stem cells from methionine adenosyl transferase 1A-deficient mice demonstrate resistance to transforming growth factor (TGF)-beta-induced apoptosis. Hepatology 2009;49:1277–1286. [PubMed: 19115422]
14. Rountree CB, Senadheera S, Mato JM, Crooks GM, Lu SC. Expansion of liver cancer stem cells during aging in methionine adenosyltransferase 1A-deficient mice. Hepatology 2008;47:1288–1297. [PubMed: 18167064]
15. Dong-Dong L, Xi-Ran Z, Xiang-Rong C. Expression and significance of new tumor suppressor gene PTEN in primary liver cancer. J Cell Mol Med 2003;7:67–71. [PubMed: 12767263]
16. Stiles B, Wang Y, Stahl A, Bassilian S, Lee WP, Kim YJ, et al. Liver-specific deletion of negative regulator Pten results in fatty liver and insulin hypersensitivity [corrected]. Proc Natl Acad Sci USA 2004;101:2082–2087. [PubMed: 14769918]
17. You H, Ding W, Rountree CB. Epigenetic regulation of cancer stem cell marker CD133 by transforming growth factor-beta. Hepatology 2010;51:1635–1644. [PubMed: 20196115]
18. Kleinman HK, Jacob K. Invasion assays. Curr Protoc Cell Biol 2001;Chapter 12 Unit 12.2.
19. Yang J, Chai L, Gao C, Fowles TC, Alipio Z, Dang H, et al. SALL4 is a key regulator of survival and apoptosis in human leukemic cells. Blood 2008;112:805–813. [PubMed: 18487508]
20. Grotegut S, von Schweinitz D, Christofori G, Lehembre F. Hepatocyte growth factor induces cell scattering through MAPK/Egr-1-mediated upregulation of Snail. EMBO J 2006;25:3534–3545. [PubMed: 16858414]
21. Osada S, Kanematsu M, Imai H, Goshima S. Clinical significance of serum HGF and c-Met expression in tumor tissue for evaluation of properties and treatment of hepatocellular carcinoma. Hepatogastroenterology 2008;55:544–549. [PubMed: 18613405]

22. Yang MH, Chen CL, Chau GY, Chiou SH, Su CW, Chou TY, et al. Comprehensive analysis of the independent effect of twist and snail in promoting metastasis of hepatocellular carcinoma. Hepatology 2009;50:1464–1474. [PubMed: 19821482]
23. Zhu Q, Xu H, Xu Q, Yan W, Tian D. Expression of Twist gene in human hepatocellular carcinoma cell strains of different metastatic potential. J Huazhong Univ Sci Technolog Med Sci 2008;28:144–146. [PubMed: 18480983]
24. Sugimachi K, Tanaka S, Kameyama T, Taguchi K, Aishima S, Shimada M, et al. Transcriptional repressor snail and progression of human hepatocellular carcinoma. Clin Cancer Res 2003;9:2657–2664. [PubMed: 12855644]
25. Jiao W, Miyazaki K, Kitajima Y. Inverse correlation between E-cadherin and Snail expression in hepatocellular carcinoma cell lines in vitro and in vivo. Br J Cancer 2002;86:98–101. [PubMed: 11857019]
26. Yan W, Fu Y, Tian D, Liao J, Liu M, Wang B, et al. PI3 kinase/Akt signaling mediates epithelial-mesenchymal transition in hypoxic hepatocellular carcinoma cells. Biochem Biophys Res Commun 2009;382:631–636. [PubMed: 19303863]
27. Stolz DB, Michalopoulos GK. Comparative effects of hepatocyte growth factor and epidermal growth factor on motility, morphology, mitogenesis, and signal transduction of primary rat hepatocytes. J Cell Biochem 1994;55:445–464. [PubMed: 7962176]
28. del Castillo G, Factor VM, Fernandez M, Alvarez-Barrientos A, Fabregat I, Thorgeirsson SS, et al. Deletion of the Met tyrosine kinase in liver progenitor oval cells increases sensitivity to apoptosis in vitro. Am J Pathol 2008;172:1238–1247. [PubMed: 18385520]
29. Balaban YH, Us D, Hascelik G, Bayraktar Y. Hepatocellular carcinoma and cholangiocarcinoma are associated with high serum levels of hepatocyte growth factor. Indian J Gastroenterol 2006;25:223–224. [PubMed: 16974053]
30. Nakanishi K, Fujimoto J, Ueki T, Kishimoto K, Hashimoto-Tamaoki T, Furuyama J, et al. Hepatocyte growth factor promotes migration of human hepatocellular carcinoma via phosphatidylinositol 3-kinase. Clin Exp Metastasis 1999;17:507–514. [PubMed: 10763917]
31. Xie Q, Liu KD, Hu MY, Zhou K. SF/HGF-c-Met autocrine and paracrine promote metastasis of hepatocellular carcinoma. World J Gastroenterol 2001;7:816–820. [PubMed: 11854908]
32. Son G, Hirano T, Seki E, Iimuro Y, Nukiwa T, Matsumoto K, et al. Blockage of HGF/c-Met system by gene therapy (adenovirus-mediated NK4 gene) suppresses hepatocellular carcinoma in mice. J Hepatol 2006;45:688–695. [PubMed: 16839638]
33. Neaud V, Faouzi S, Guirouilh J, Monvoisin A, Rosenbaum J. Hepatocyte growth factor secreted by human liver myofibroblasts increases invasiveness of hepatocellular carcinoma cells. Curr Top Pathol 1999;93:195–203. [PubMed: 10339912]
34. Guirouilh J, Le Bail B, Boussarie L, Balabaud C, Bioulac-Sage P, Desmouliere A, et al. Expression of hepatocyte growth factor in human hepatocellular carcinoma. J Hepatol 2001;34:78–83. [PubMed: 11211911]
35. Breuhahn K, Longerich T, Schirmacher P. Dysregulation of growth factor signaling in human hepatocellular carcinoma. Oncogene 2006;25:3787–3800. [PubMed: 16799620]
36. Chaffer CL, Brennan JP, Slavin JL, Blick T, Thompson EW, Williams ED. Mesenchymal-to-epithelial transition facilitates bladder cancer metastasis: role of fibroblast growth factor receptor-2. Cancer Res 2006;66:11271–11278. [PubMed: 17145872]
37. Bonneton C, Sibarita JB, Thiery JP. Relationship between cell migration and cell cycle during the initiation of epithelial to fibroblastoid transition. Cell Motil Cytoskeleton 1999;43:288–295. [PubMed: 10423270]
38. Poon RT, Ng IO, Lau C, Yu WC, Fan ST, Wong J. Correlation of serum basic fibroblast growth factor levels with clinicopathologic features and postoperative recurrence in hepatocellular carcinoma. Am J Surg 2001;182:298–304. [PubMed: 11587697]

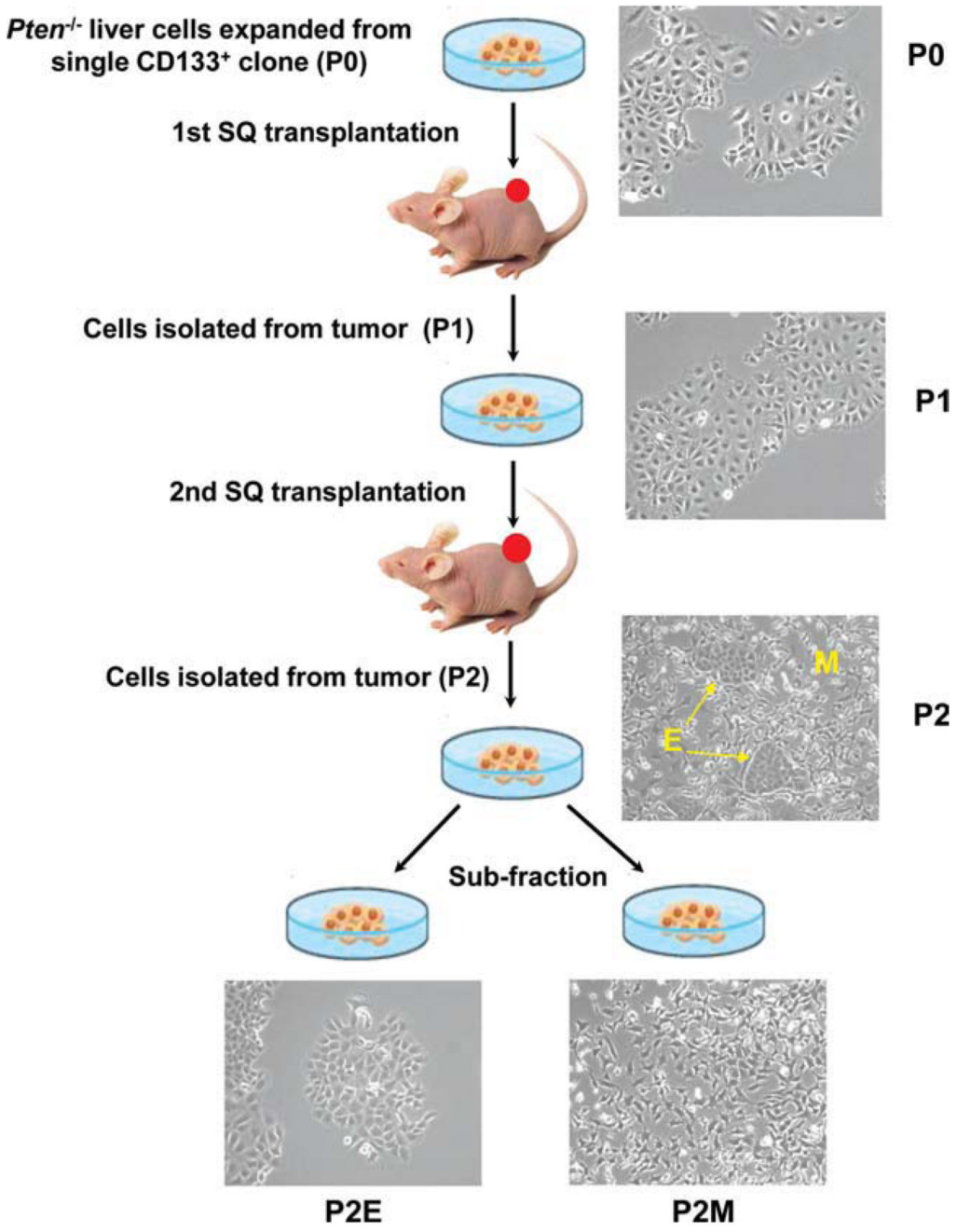

Fig. 1.

Diagram of cell derivation process. *Pten*$^{-/-}$ tumor cells acquired EMT after two rounds of subcutaneous transplantation in nude mice. The parent cell line P0 demonstrates epithelial cell morphology. Two distinct cell types are observed within P2: epithelial and mesenchymal. Epithelial cells had a cobblestone morphology with tight cell–cell contacts, similar to P0 cells. Mesenchymal cells had elongated, spindle-like morphology. P2 epithelial (P2E) and mesenchymal (P2M) phenotype cells were subfractionated.

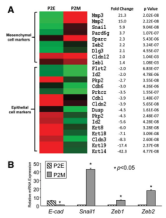

Fig. 2.

EMT microarray data set. (A) Hierarchy clustering of statistically significant EMT-associated genes further confirmed that P2 cells acquired EMT. Several epithelial cell markers such as *E-cadherin, Claudin3* (*Cldn3*), *keratins* (*Krt8*, *Krt14*, *Krt18*, and *Krt19*), and *Plakophilin 2* (*Pkp2*) were significantly down-regulated, whereas several mesenchymal cell markers, matrix metalloproteinases (*Mmp2/3*), and EMT-related transcription factors (*Snail1*, *Zeb1*, and *Zeb2*) were up-regulated in P2M cells compared with P2E cells. Raw intensity values are graphed. A single-sample *t* test was performed and *P* values were calculated using a TIGR MultiExperiment Viewer (n = 4 sequential passages/group; full data set available at http://www.ncbi.nlm.nih.gov/geo, accession #GSE18255). (B) Validation of EMT markers using real-time reverse-transcription PCR showing that *E-cadherin* was significantly down-regulated and that EMT-related transcription factors, *Snail1*, *Zeb1*, and *Zeb2*, were significantly up-regulated in P2M mesenchymal cells (n = 3, mean ± SD). **P* < 0.05.

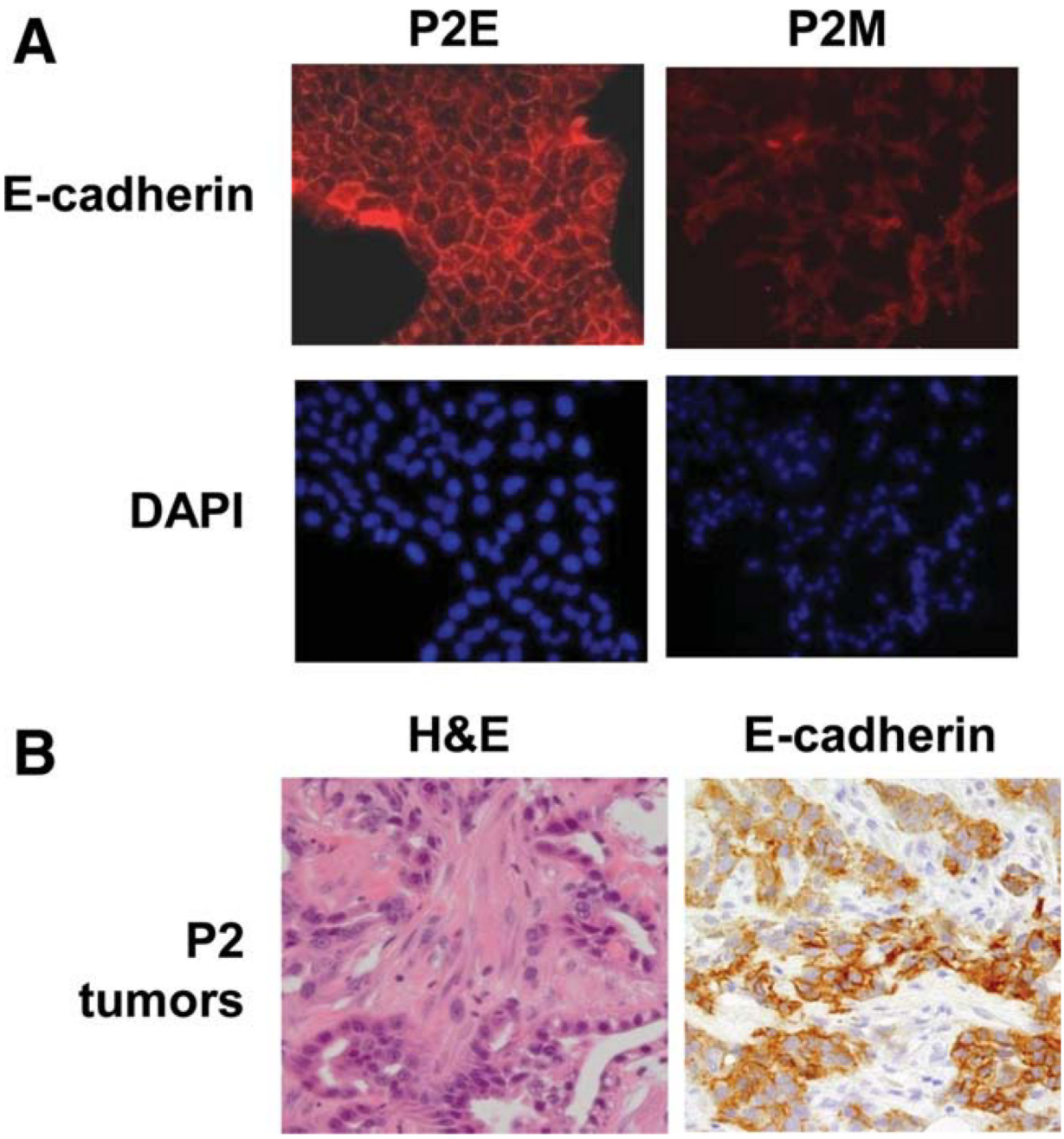

Fig. 3.
Confirmation of EMT in P2 tumors. (A) Immunofluorescent staining for E-cadherin confirms the mesenchymal phenotype of P2M cells. (B) Representative hematoxylin-eosin staining and immunohistochemical staining with E-cadherin in P2 tumor with mixed epithelial and mesenchymal morphology.

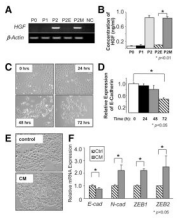

Fig. 4.

HGF was secreted by mesenchymal cells and induced EMT in P2E cells. (A) High expression levels of HGF were detected in both P2 and P2M cells using semiquantitative reverse-transcription PCR. (B) HGF, detected by means of enzyme-linked immunosorbent assay, was secreted into CM of P2M cells (n = 3, mean ± SD). **P* < 0.01 versus P2E. (C) Recombinant HGF (5 ng/mL) promoted P2E cells undergoing EMT, showing morphological change and (D) recombinant HGF promoted the down-regulation of E-cadherin (n = 3, mean ± SD). **P* < 0.05. (E) Cuboidal and cobblestone epithelial cells shifted to spindle-like mesenchymal cells when P2E cells were treated with CM collected from P2M after 24 hours of SF medium incubation. (F) CM collected from P2M cells induced P2E cells undergoing EMT, showing that E-cadherin was down-regulated but N-cadherin, Zeb1, and Zeb2 were significantly up-regulated (n = 3, mean ± SD). **P* < 0.05 versus SF control.

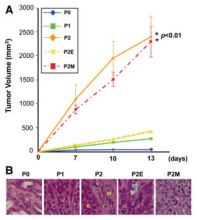

Fig. 5.

P2M cells exhibited aggressive growth in vivo. (A) Volumetric analysis demonstrates significant tumor growth of P2 and P2M cells (n = 4 mice/group, mean ± SD). **P* < 0.01 versus P0. (B) Histological examination demonstrates that P1 and P2E cells developed uniform hepatoma-like tumors, whereas P2M cells formed fibroblastoma-like neoplasms, and tumors initiated by P2 cells mixed with both epithelial and mesenchymal cell morphology (hematoxylin-eosin staining).

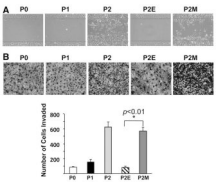

Fig. 6.

Mesenchymal cells migrate and invade in vitro. (A) Wound healing assay demonstrates that there are significantly more mesenchymal cells that migrate into the wound area compared with their epithelial counterparts. (B) Matrigel assay reveals a significant number of P2M cells invading through pores (n = 3, mean cells/field ± SD). **P* < 0.01 versus P2E.

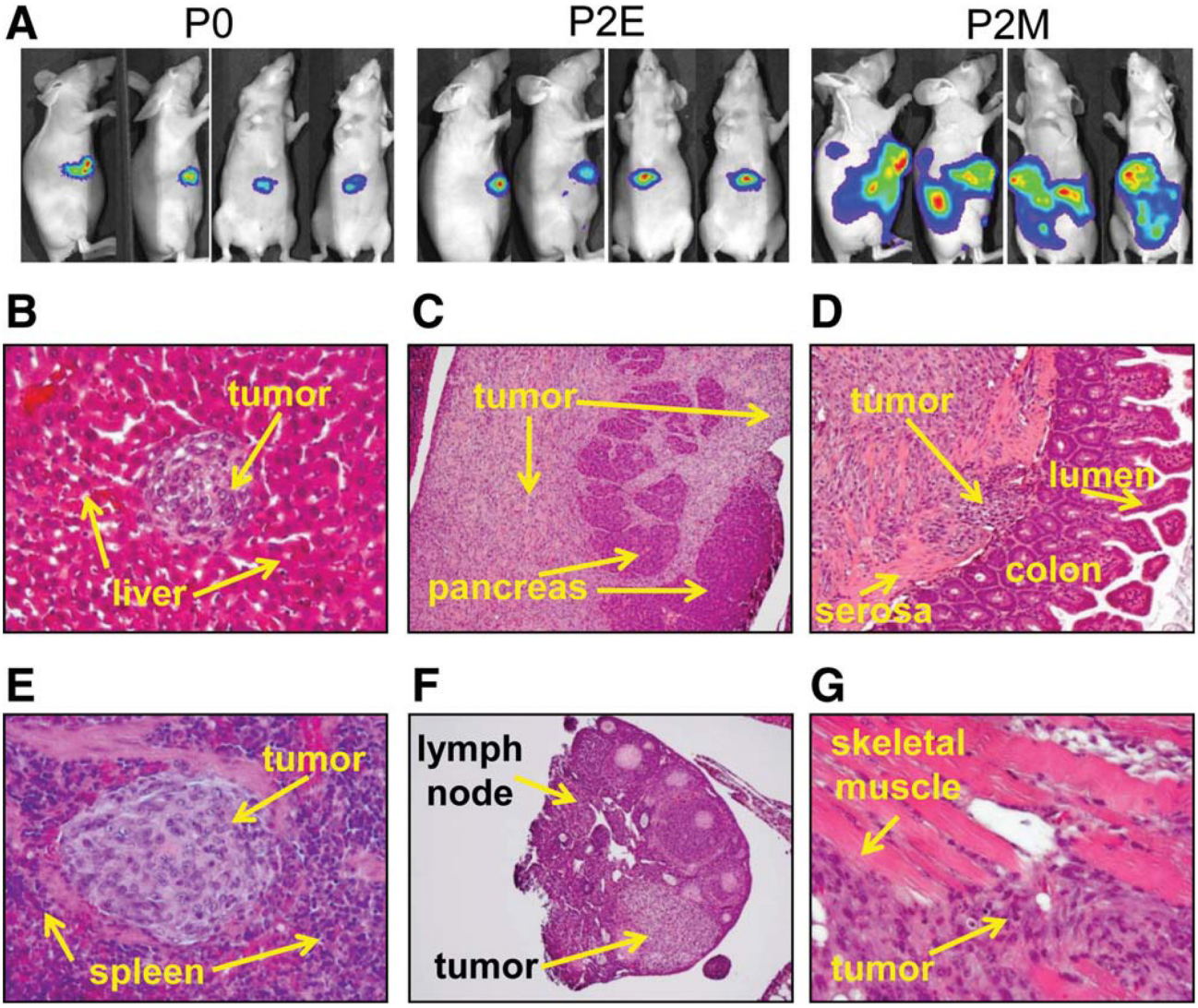

Fig. 7.

Mesenchymal cells migrate and invade abdominal organs in vivo. Acquisition of EMT promoted tumor invasion in nude mice that were orthotopically transplanted with P0, P2E, and P2M cells, respectively. (A) Bioluminescent images demonstrate that P2M tumor cells spread to the peritoneal cavity and invaded multiple organs, whereas P0 and P2E tumor growth was restricted to the livers (n = 5 mice/group, representative anterior–posterior and lateral images; exposure time, 1 minute for P0 and P2E and 5 seconds for P2M). (B–G) Hematoxylin-eosin staining results showed intrahepatic metastasis (B) and invasion of pancreas acinar tissue (C), colonic mucosa (D), spleen (E), peritoneal lymph nodes (F), and skeletal muscle of anterior abdominal wall (G) from P2M-derived tumors.